
Energy-Based Imitation Learning

Minghuan Liu, Tairan He, Minkai Xu, Weinan Zhang

Shanghai Jiao Tong University

{minghuanliu,wnzhang}@sjtu.edu.cn, {tairanhe,mkxu}@apex.sjtu.edu.cn

Abstract

We tackle a common scenario in imitation learning (IL), where agents try to recover the optimal policy from expert demonstrations without further access to the expert or environment reward signals. The classical inverse reinforcement learning (IRL) solution involves bi-level optimization and is of high computational cost. Recent generative adversarial methods formulate the IL problem as occupancy measure matching, which, however, suffer from the notorious training instability and mode-dropping problems. Inspired by recent progress in energy-based model (EBM), in this paper, we propose a novel IL framework named Energy-Based Imitation Learning (EBIL), solving the IL problem via estimating the expert energy as the surrogate reward function through score matching. EBIL combines the idea of both EBM and occupancy measure matching, which enjoys: (1) high model flexibility for expert policy distribution estimation; (2) efficient computation that avoids the previous alternate training fashion. Though motivated by matching the policy between the expert and the agent, we surprisingly find a non-trivial connection between EBIL and the classic Max-Entropy IRL (MaxEnt IRL) approach, and further show that EBIL can be seen as a simpler and more efficient solution of MaxEnt IRL. Extensive experiments show that EBIL can always achieve comparable performance against state-of-the-art methods with less computation cost.

1 Introduction

Reinforcement Learning (RL) has demonstrated its effectiveness in a variety of tasks [27, 30, 21]. However, a common challenge for RL methods is their severe dependency on a well-designed reward signal. Fortunately, the reward signals will be unnecessary if we consider to Learn from Demonstrations (LfD), or commonly known as Imitation Learning (IL) [20]. In this paper, we focus on the common setting of IL, where agents learn their policies from the samples of trajectories from the expert, without any further access to the expert or explicit rewards.

Classic solutions for IL such as behavior cloning (BC) [31] aim to minimize 1-step deviation error along the provided expert trajectories with supervised learning, which suffers seriously from an extensive collection of expert data and compounding error caused by covariate shift [35, 36]. As an alternative, Inverse Reinforcement Learning (IRL) [28, 1] tries to recover a reward function from the expert and subsequently train an RL policy under that, yet such a bi-level optimization scheme can result in high computational cost. The recent solution as GAIL [19] derived from Max-Entropy IRL (MaxEnt IRL) formulates the IL problem as occupancy measure matching. GAIL takes advantage of GAN [13] to minimize the Jensen-Shannon divergence between the agent’s occupancy measures and the expert’s while it also inherits the notorious defects of GAN, including training instability and mode dropping [5].

Analogous to IL, learning statistical models from given data and generating similar samples has been an important topic in generative model community. Among them, recent energy-based models (EBMs) have gained much attention because of the simplicity and flexibility in likelihood estima-

tion [9, 42]. In this paper, we propose to leverage the advantages of EBMs to solve IL with a novel framework called Energy-Based Imitation Learning (EBIL), which addresses the problem via expert energy estimation in a two-step fashion: first estimates an unnormalized probability density (*a.k.a.* energy) of expert’s occupancy measure through score matching, and then takes the energy to construct a surrogate reward function as a guidance for the agent to learn the desired policy. In experiments, we first verify our idea in a simple one-dimensional environment by visualizing the estimated reward and the induced policy; then we evaluate our algorithm on extensive high-dimensional continuous control benchmarks, showing that EBIL can always achieve comparable or better performance than state-of-the-art methods.

In addition to the stability and flexibility of EBMs, EBIL also enjoys a more efficient training procedure thanks to the two-step training fashion that overcome the undesired slow alternate training process as in IRL and GAIL. Though the underlying intuition behind our proposed methodology was to match the expert’s occupancy measure through EBM, we surprisingly find that there indeed exists a non-trivial connection between our method and previous MaxEnt IRL methods. Thus we further provide a theoretical illustration of the relation between EBIL and MaxEnt IRL. Specifically, we show that EBIL is a dual problem of MaxEnt IRL and is also a simplified and efficient solution for it. The analysis, along with past works provides a holistic view of the role of EBM in imitation learning.

2 Preliminaries

In this section, we present the definition of reinforcement learning problem, imitation learning and energy-based models along with the notations.

2.1 Maximum Entropy Reinforcement Learning

Reinforcement Learning (RL) problems can be seen as Markov Decision Process (MDP), which is represented as a tuple $\mathcal{M} = \langle \mathcal{S}, \mathcal{A}, P, \rho_0, r, \gamma \rangle$, where \mathcal{S} is the set of states, \mathcal{A} represents the action space of the agent, $P : \mathcal{S} \times \mathcal{A} \times \mathcal{S} \rightarrow \mathbb{R}$ is the state transition probability distribution, $\rho_0 : \mathcal{S} \rightarrow \mathbb{R}$ is the distribution of the initial state s^0 , and $\gamma \in [0, 1]$ is the discounted factor. The agent holds its policy $\pi(a|s) : \mathcal{S} \times \mathcal{A} \rightarrow [0, 1]$ to make decisions and receive rewards defined as $r : \mathcal{S} \times \mathcal{A} \rightarrow \mathbb{R}$. For an arbitrary function $f : \langle s, a \rangle \rightarrow \mathbb{R}$, it is easy to show that $\mathbb{E}_\pi[f(s, a)] = \mathbb{E}_{s \sim P, a \sim \pi}[f(s, a)] \triangleq \mathbb{E}[\sum_{t=0}^{\infty} \gamma^t f(s_t, a_t)]$, where $s_0 \sim \rho_0$, $a_t \sim \pi(\cdot|s_t)$, $s_{t+1} \sim P(\cdot|a_t, s_t)$.

The normal objective of RL is to get an optimal policy such that it can maximize its own total expected return $R \triangleq \mathbb{E}_\pi[r(s, a)] = \mathbb{E}[\sum_{t=0}^{\infty} \gamma^t r(s_t, a_t)]$, while Maximum Entropy Reinforcement Learning (MaxEnt RL) augments the objective with an entropy term to find a stochastic policy that can also maximize its entropy at each visited state [19, 16] as:

$$\pi^* = \arg \max_{\pi} \mathbb{E}_\pi[r(s, a)] + \alpha H(\pi), \quad (1)$$

where $H(\pi) \triangleq E_\pi[-\log \pi(a|s)]$ is the γ -discounted causal entropy [2] and the temperature hyper-parameter α is used to determine the relative importance of entropy as a reward, we will let $\alpha = 1$ by default in the following part of this paper.

Occupancy Measure. The agent generates trajectories, *i.e.*, state-action (s, a) pairs when they interact with the environment with policy π lead to the definition of occupancy measure $\rho_\pi^{s,a}(s, a)$ or $\rho_\pi^s(s)$ as the density of occurrence of states or state-action pairs:

$$\begin{aligned} \rho_\pi^{s,a}(s, a) &= (1 - \gamma) \sum_{t=0}^{\infty} \gamma^t P(s_t = s, a_t = a | \pi) \\ &= \pi(a|s)(1 - \gamma) \sum_{t=0}^{\infty} \gamma^t P(s_t = s | p, \pi) = \pi(a|s)\rho_\pi^s(s), \end{aligned} \quad (2)$$

which allows us to write that: $\mathbb{E}_\pi[\cdot] = \sum_{s,a} \rho_\pi(s, a)[\cdot] = \mathbb{E}_{(s,a) \sim \rho_\pi^{s,a}}[\cdot]$. For simplicity, we will denote $\rho_\pi^{s,a}$ as ρ_π without further explanation in the following sections, and we have $\rho_\pi \in \mathcal{D} \triangleq \{\rho_\pi : \pi \in \Pi\}$.

2.2 Imitation Learning

Imitation learning (IL) [20] studies the task of Learning from Demonstrations (LfD), which aims to learn a policy from expert demonstrations which typically consists the expert trajectories interacted with environments without receiving reward signals from environments. General IL objective tries to minimize the distance between the actions taken by policy π and expert policy π_E :

$$\pi^* = \arg \min_{\pi} \mathbb{E}_{s \sim \rho_{\pi}^s} [\ell(\pi(\cdot|s), \pi_E(\cdot|s))], \quad (3)$$

where ℓ denotes some distance metric. However, as we do not ask the expert agent for further demonstrations, it is always hard to optimize Eq. (3) with only expert trajectories accessible. Thus, Behavior Cloning (BC) [31] provides a straightforward method by learning the policy in a supervised way, where the objective is represented as a Maximum Likelihood Estimation (MLE):

$$\hat{\pi}^* = \arg \min_{\pi} \mathbb{E}_{s \sim \rho_{\pi_E}^s} [\ell(\pi_E(\cdot|s), \pi(\cdot|s))], \quad (4)$$

which suffers from covariate shift problem for the i.i.d. state assumption.

Another branch of methods are under the basic idea of Inverse Reinforcement Learning (IRL) [28] that tries to recover the reward function r^* in the environments. An underlying assumption of IRL is that the reward function r^* will evaluate the expert policy as the optimal policy in the environment. Formally,

$$\pi^* = \arg \max_{\pi} \mathbb{E}_{(s,a) \sim \rho_{\pi}} [r^*(s, a)], \quad (5)$$

which suffers typically from a high complexity for its bi-level optimization and can cause ambiguity resulting in different reward functions.

Derived from Max-Entropy IRL (MaxEntIRL) which solves the ambiguity of normal IRL methods, generative Adversarial Imitation Learning (GAIL) [19] shows that the objective of MaxEntIRL is a dual problem of occupancy measure matching, and thus can be solved through generative models such as GAN. Specifically, it shows that the policy learned by RL on the reward recovered by IRL can be characterized by

$$\text{RL} \circ \text{IRL}_{\psi}(\pi_E) = \arg \min_{\pi} -H(\pi) + \psi^*(\rho_{\pi} - \rho_{\pi_E}), \quad (6)$$

where ψ is the regularizer, and $f^* : \mathbb{R}^{\mathcal{S} \times \mathcal{A}} \rightarrow \overline{\mathbb{R}}$ is the convex conjugate for an arbitrary function $f : \mathbb{R}^{\mathcal{S} \times \mathcal{A}} \rightarrow \overline{\mathbb{R}}$ given by $f^*(x) = \sup_{y \in \mathbb{R}^{\mathcal{S} \times \mathcal{A}}} x^T y - f(y)$. Eq. (6) shows that various settings of ψ , which can be seen as a distance metric leading to various solutions of imitation learning.

2.3 Energy-Based Models

For a random variable $X \sim p(x)$, energy-based model (EBM) [24] builds the density of data by estimating the energy function $E(x)$ with sample x as

$$p(x) = \frac{1}{Z} \exp(-E(x)), \quad (7)$$

where $Z = \int \exp(-E(x)) dx$ is the partition function, which is normally intractable to compute exactly for high-dimensional x . The energy function E can be seen as the unnormalized log-density of data which is always optimized to maximize the likelihood of the data. Typically, the estimation of the partition function Z is computationally expensive, which requires sampling from the Boltzmann distribution $p(x)$ within the inner loop of learning.

3 Imitation Learning via Expert Energy Estimation

In this section, we provide an energy-based perspective of IL and propose to learn the agent’s policy via estimating the energy of the expert demonstrations.

3.1 Energy-Based Imitation Learning

IL requires to recover expert policy π_E from static demonstrations which consists of expert trajectories and cannot be further expanded by interacting with the expert agent. Instead of minimizing

the distance between every action taken by agent policy and expert's based on expert trajectories as shown in Eq. (3), or find the policy which is optimal that achieves the maximum accumulated reward under unknown reward function, Eq. (6) prescribes that we are able to formulate the problem of recovering expert policy based on its occupancy measure. Formally, denoting the set of policies as Π and the set of valid occupancy as measures $\mathcal{D} \triangleq \{\rho_\pi > 0 : \pi \in \Pi\}$, Lemma 1 shows the one-to-one correspondence between Π and \mathcal{D} :

Lemma 1 (Theorem 2 of [43]). *If $\rho \in \mathcal{D}$, then ρ is the occupancy measure for $\pi_\rho(a|s) \triangleq \frac{\rho(s,a)}{\sum_{a'} \rho(s,a')}$, and π_ρ is the only policy whose occupancy measure is ρ .*

Thus, the occupancy measure can be used as an alternative in the general IL objective shown in Eq. (3). Applying the reverse KL divergence as the distance metric, we could construct the IL objective as minimizing the KL divergence D_{KL} of the occupancy measures between agent's policy and expert's:

$$\pi^* = \arg \min_{\pi} D_{KL}(\rho_\pi \| \rho_{\pi_E}) . \quad (8)$$

Proposition 1. *The optimal solution for the reverse KL divergence objective of IL shown in Eq. (8) is that $\pi^* = \pi_E$.*

Proof. It is obvious that the solution of Eq. (8) is unique since D_{KL} is convex for ρ_π , which achieves the optimal value iff $\rho_\pi = \rho_{\pi_E}$. According to Lemma 1, we can recover policy π_E if we can recover the occupancy measure of expert policy. Thus the optimal solution is that $\pi^* = \pi_E$. \square

Considering to model the occupancy measure with Boltzmann distribution, the density can be represented by an EBM as

$$\rho_\pi(s, a) = \frac{1}{Z} \exp(-E(s, a)) , \quad (9)$$

where leads to the following proposition.

Proposition 2. *The reverse KL divergence objective of IL Eq. (8) is equivalent to the following of Energy-Based Imitation Learning (EBIL) objective Eq. (10):*

$$\pi^* = \arg \max_{\pi} \mathbb{E}_{\pi} [-E_{\pi_E}(s, a)] + H(\pi) . \quad (10)$$

The proof of Proposition 2 is in Appendix B.1. Notice that Eq. (10) provides exactly the same form as the objective of MaxEnt RL shown in Eq. (1), and thus it is natural to associate the reward function with the energy-based model of experts $r(s, a) = -E_{\pi_E}(s, a)$ ¹. Generally, we can choose the reward function as $h(-E_{\pi_E}(s, a))$ where h is a monotonically increasing linear function to keep the objective of Eq. (10) still true.

Therefore, EBIL that learns with MaxEnt RL using the expert energy function as the reward function aims to minimize the reverse KL divergence between the agent's occupancy measure and the expert's. It is worth noting that if we treat EBIL learning procedure with a standard RL objective without the entropy term, then this objective will collapse into minimizing the cross entropy of the occupancy measure rather than the KL divergence.

3.2 Expert Energy Estimation with Demonstrations

As described above, our reward function is determined by $E_{\pi_E}(s, a)$, a learned energy function of the occupancy measure. In this section, we elaborate on how to estimate $E_{\pi_E}(s, a)$ from expert demonstrations. Specifically, in this paper, we leverage Deep Energy Estimator Networks (DEEN) [39], a scalable and efficient algorithm to directly estimate the energy of expert's occupancy measure of policy via a differentiable framework. Then we can take the estimated energy as the surrogate reward to train the agent policy.

Formally, let the random variable $X = g(s, a) \sim g(\rho_{\pi_E}(s, a))$. Let the random variable Y be the noisy observation of X that $y \sim x + N(0, \sigma^2 I)$, e.g., y is derived from samples x by adding with

¹One may notice that according to Lemma 1, we can simply recover the expert policy directly through $\pi^* = \exp(-E(s, a)) / \sum_{a'} \exp(-E(s, a'))$. However, this may be hard to generalize to continuous or high-dimensional action space in practice. For more discussions one can refer to Section D.2.

white Gaussian noise $\xi \sim N(0, \sigma^2 I)$. The empirical Bayes least square estimator, *i.e.*, the optimal denoising function $g(y)$ for the white Gaussian noise, is solved as

$$g(y) = y + \sigma^2 \nabla_y \log p(y). \quad (11)$$

Such a function can be trained with a feedforward neural network \hat{g} by denoising each sample $y_i \in Y$ to recover $x_i \in X$, which can be implemented with a Denoising Autoencoder (DAE) [45]. Then we can use the DAE \hat{g} to approximate the score function $\nabla_y \log p(y)$ of the corrupted distribution by $\nabla_y \log p(y) \propto \hat{g}(y) - y$ [34, 26, 32]. However, one should note that the DAE does not provide the energy function but instead approximates the score function – the gradient of $\log \rho_\pi(s, a)$, which cannot be adopted as the vital reward function.

Thus, in order to estimate the EBM of expert’s state-action pairs provided through demonstration data, we consider to parameterize the energy function $E_\theta(y)$ with a neural network explicitly. As shown in [39], such a network called DEEN can be trained by minimizing the following objective:

$$\arg \min_{\theta} \sum_{x_i \in X, y_i \in Y} \left\| x_i - y_i + \sigma^2 \frac{\partial E_\theta(y = y_i)}{\partial y} \right\|^2, \quad (12)$$

which ensures the relation of score function $\partial E_\theta(y)/\partial y$ shown in Eq. (11). It is worth noting that the EBM estimates the energy of the noisy samples. This can be seen as a Parzen window estimation of $p(x)$ with variance σ^2 as the smoothing parameter [38, 44]. A trivial problem here is that Eq. (12) requires the samples (state-action pairs) to be continuous so that the gradient can be accurately computed. Actually, EBIL can be easily expanded to discrete space by using other energy estimation methods, *e.g.*, Noise Contrastive Estimation [14]. In this work, we concentrate on the continuous space and leave the discrete version in the future.

In practice, we learn the EBM of expert data from off-line demonstrations and construct the reward function, which will be fixed until the end to help agent learn its policy with a normal RL procedure. Specifically, we construct the surrogate reward function $\hat{r}(s, a)$ as follows:

$$\hat{r}(s, a) = h(-E_{\pi_E}(s, a)), \quad (13)$$

where $h(x)$ is a monotonically increasing linear function, which can be specified for different environments. Formally, the overall EBIL algorithm is presented in Algo. 1 of Appendix A.

4 Discussions

In this paper, we propose to estimate the energy function from expert demonstrations directly, then regard it as the surrogate reward function to force the agent to learn a good policy that can match the occupancy measure of the expert. Interestingly, MaxEnt IRL can be seen as a special implementation of EBM, which constructs the expert demonstrations as a Boltzmann distribution of the cost / reward function, and tries to extract optimal policy from it. In this section, we theoretically clarify the relation between EBIL and MaxEnt IRL, and show that EBIL actually can be seen as a simplified and efficient solution for MaxEnt IRL.

IRL aims to recover a cost or reward, under which the set of demonstrations are near-optimal. However, the optimal solution is still underdefined. To that end, MaxEnt IRL resolves the reward ambiguity problem in normal IRL by employing the principle of maximum entropy [48, 47, 2], which introduces probabilistic models to explain suboptimal behaviors as noise. More specifically, MaxEnt IRL models the paths in demonstrations using a Boltzmann distribution, where the energy is given by the unknown reward function \hat{r}^* :

$$p_{\hat{r}}(\tau) = \frac{1}{Z} \exp(\hat{r}^*(\tau)), \quad (14)$$

where $\tau = \{s_0, a_0, \dots, s_T, a_T\}$ is a trajectory of state-action pairs and T is its length; $\hat{r}^*(\tau) = \sum_t \hat{r}^*(s_t, a_t)$ is the reward function, under which the expert demonstrations are optimal; Z is the partition function.² Similar to other EBMs, the parameters of the reward function is optimized to maximize the likelihood of expert trajectories.

²Note that Eq. (14) is formulated under the deterministic MDP setting. A general form for stochastic MDP is derived in [48, 47] yet owns similar analysis: the probability of a trajectory is decomposed as the product of conditional probabilities of the states s_t , which can factor out of all likelihood ratios since they are not affected by the reward function.

Under this model, ultimately we hope that our policy can generate any trajectories with the probability increases exponentially as the return gets higher, and we can obtain the desired optimal trajectories with the highest likelihood. Following previous work, we focus on the maximum causal entropy IRL [48, 47], which aims to maximize the entropy of the distribution over paths under the constraints of feature matching that can be regarded as the matching of the rewards. Formally, maximum causal entropy IRL can be represented as the following optimization problem [19]:

$$\hat{r}^* = \arg \max_{\hat{r}} \mathbb{E}_{\pi_E} [\hat{r}(s, a)] - \left(\max_{\pi \in \Pi} \mathbb{E}_{\pi} [\hat{r}(s, a)] + H(\pi) \right), \quad (15)$$

where $H(\pi) := \mathbb{E}_{\pi} [-\log \pi(a|s)]$ is the causal entropy [2] of the policy π .

4.1 EBIL is a Dual Problem of MaxEnt IRL

Now we first illustrate that EBIL (Eq. (8)) is a dual of the above MaxEnt IRL problem. The proof sketch is to show that EBIL is a instance of occupancy measure matching problem which has been proven to be a dual problem of MaxEnt IRL.

Lemma 2. *IRL is a dual of the following occupancy measure matching problem and the induced optimal policy is the primal optimum which matches the expert's occupancy measure ρ_{π_E} :*

$$\min_{\rho_{\pi} \in \mathcal{D}} \bar{H}(\rho_{\pi}) \text{ subject to } \rho_{\pi}(s, a) = \rho_{\pi_E}(s, a) \forall s \in \mathcal{S}, a \in \mathcal{A}. \quad (16)$$

Proposition 3. *The EBIL objective Eq. (8) is an instance of the occupancy measure matching problem Eq. (16).*

The proof of Lemma 2 can be refered to the Section 3 of [19], and the proof of Proposition 3 is shown in Appendix B.2. Combining Lemma 2 and Proposition 3, we have that EBIL is a dual problem of MaxEnt IRL.

4.2 EBIL is More Efficient than IRL

Now we are going to illustrate why EBIL is a more efficient solution. Recall that the intuition of MaxEnt IRL is to regard the demonstrations as a Boltzmann distribution of the reward function, and then induce the optimal policy. Suppose that we have already recovered the optimal reward function \hat{r}^* , then the optimal policy is induced by the following practical forward MaxEnt RL procedure:

$$\pi^* = \arg \max_{\pi} \mathbb{E}_{\pi} [\hat{r}^*(s, a)] + H(\pi). \quad (17)$$

Now we further demonstrate that EBIL aims to seek the same policy, while through a simplified and more efficient training procedure.

Proposition 4. *Denote τ and τ_E are trajectories sampled by the agent and the expert respectively, and suppose we have the optimal reward function \hat{r}^* , then the policy π^* induced by \hat{r}^* is the optimal solution to the following optimization problem:*

$$\min_{\pi} D_{KL}(p(\tau) \| p(\tau_E)). \quad (18)$$

Proposition 5. *The optimization problem Eq. (18) is equivalent to the KL divergence IL objective Eq. (8) and the EBIL objective Eq. (10).*

The proof for these two propositions are in Appendix B.3 and Appendix B.4 separately. These two propositions together reveal the optimal policy obtained from EBIL is the same as the one from MaxEnt IRL when the optimal reward function is recovered. However, the latter one is indirect and much more computationally expensive. Primitively, as shown in Eq. (15), IRL methods aim to recover the optimal reward function instead of directly learn the policy, requiring estimating the partition function Z , which is hard, especially in high-dimensional spaces. By contrast, EBIL seeks to directly learn the policy guided by the estimated expert energy of occupancy measure, which is much more efficient.

As a supplementary statement, [10] reveals the close relationship between Guided Cost Learning [11] (a sample-based algorithm of MaxEnt IRL) and GAIL. Besides, [12] also presents a unified perspective among previous IL algorithms and discuss in a divergence minimization view similar as ours shown in Section 3.1. Therefore, all of these methods show connections among each other.

5 Related Work

Instead of seeking to alternatively update the policy and the reward function as in IRL and GAIL, many recent works of IL aim to learn a fixed reward function directly from expert demonstrations and then apply a normal reinforcement learning procedure with that reward function. This is first proposed by Random Expert Distillation (RED) [46], which employs the idea of Random Network Distillation [6] to estimate the support of expert policy, and compute the reward function by the loss of fitting a random neural network. In addition, Disagreement-Regularized Imitation Learning [4] constructs the reward function using the disagreement in their predictions of an ensemble of policies trained on the demonstration data, which is optimized together with a supervised behavioral cloning cost. Instead of using a learned reward function, the fixed reward of Soft-Q Imitation Learning [33] applies constant rewards by setting positive rewards for the expert state-actions and zero rewards for other ones, which is optimized with the off-policy SQL algorithm [17].

Our EBIL relies highly on EBMs, which have played an important role in a wide range of tasks including image modeling, trajectory modeling and continual online learning [8]. Thanks to the appealing features, EBMs have been introduced into many RL literature, for instance, parameterized as value function [37], employed in the actor-critic framework [18], applied to MaxEnt RL [16] and used to model regularization in model-based RL planning [3]. [10] also reveals the connection between IRL and EBMs. However, EBMs are always difficult to train due to the partition function [10]. Nevertheless, recent works have tackled the problem of training large-scale EBMs on high-dimensional data, such as DEEN [39] which is also the method we applied in our algorithm. Except for DEEN, there still leaves plenty of choices for efficiently training EBMs [15, 8, 29].

6 Experiments

6.1 Synthetic Task

In the synthetic task, we want to evaluate the qualitative performance of different IL methods by displaying the heat map of the learned reward and sampled trajectories. As analyzed in Section 3 and 4, EBIL is capable of guiding the agent to recover the expert policy and correspondingly generate the high-quality trajectories. To demonstrate this point, we evaluate EBIL along with its counterparts (GAIL [19], GMMIL³ [22] and RED [46]) on a synthetic environment where the agent tries to move in a one-dimensional space. Specifically, the state space is $[-0.5, 10.5]$ and the action space is $[-1, 1]$. The environment initializes the state at 0, and we set the expert policy as static rule policies $\pi_E = \mathcal{N}(0.25, 0.06)$ when the state $s \in [-0.5, 5]$, and $\pi_E = \mathcal{N}(0.75, 0.06)$ when $s \in [5, 10.5]$. The sampled expert demonstration contains 40 trajectories with up to 30 timesteps in each one. For all methods, we choose SAC [17] as the learning algorithm.

We plot the KL divergence between the agent’s and the expert’s trajectories during the training procedure in Fig. 1 and visualize the final estimated rewards with corresponding induced trajectories in Fig. 2. As illustrated in Fig. 2(b) and Fig. 1, the reward estimated by EBIL successfully captures the likelihood of the expert trajectories, and the induced policy quickly converge to the expert policy. By contrast, GAIL requires a noisy adversarial process to correct the policy. As a result, although GAIL achieves compatible final performance against EBIL (Fig. 2(c)), it suffers a slow, unstable training as shown in Fig. 1 and assigns arbitrary reward for some regions of the state-action space. In addition, as suggested in Fig. 2(d) and Fig. 2(e) respectively, GMMIL is not effective enough in this simple one-dimensional domain with the meaningless reward, and RED suffers from the diverged reward and fail to precisely imitate the expert.

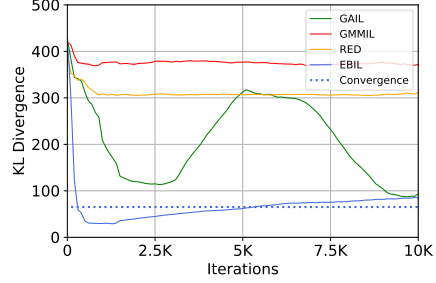


Figure 1: The KL divergence between the agent trajectories and the expert during the learning procedure, which indicates that EBIL is much more stable than the other methods. The blue dash line represents the converged result of EBIL.

³GMMIL utilizes the maximum mean discrepancy as the distance metric to guide the agent training, motivated by Generative Moment Matching Network (GMMN) [25].

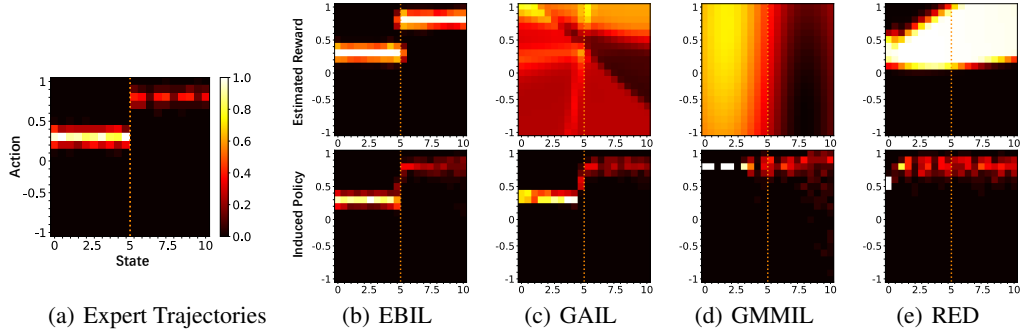


Figure 2: Heat maps of the expert trajectories (leftmost), the *estimated reward* signals recovered by different methods (top) and the *induced policy* corresponding to each reward (bottom). The horizontal axis is the *state space*, and the vertical axis is the *action space*. The red dotted line represents the position where the agent should change its policy. It is worth noting that EBIL and RED both own fixed reward functions, while GAIL and GMMIL iteratively update the reward signals. We do not compare BC since it learns the policy via supervised learning, and thus no reward signal is recovered.

Table 1: Comparison for different methods of the episodic true rewards on 5 continuous control benchmarks. The means and the standard deviations are evaluated over 50 runs.

	Humanoid	Hopper	Walker2d	Swimmer	InvertedDoublePendulum
Random	100.38 ± 28.25	14.21 ± 11.20	0.18 ± 4.35	0.89 ± 10.96	49.57 ± 16.88
BC	178.74 ± 55.88	28.04 ± 2.73	312.04 ± 83.83	5.93 ± 16.77	138.81 ± 39.99
GAIL	145.84 ± 7.01	459.33 ± 216.79	278.93 ± 36.82	23.79 ± 21.84	122.71 ± 71.36
GMMIL	416.83 ± 59.46	1000.87 ± 0.87	1585.91 ± 575.72	-0.73 ± 3.28	4244.63 ± 3228.14
RED	140.23 ± 19.10	641.08 ± 2.24	641.13 ± 2.75	-3.55 ± 5.05	6400.19 ± 4302.03
EBIL (Ours)	472.22 ± 107.72	1040.99 ± 0.53	2334.55 ± 633.91	58.09 ± 2.03	8988.37 ± 1812.76
Expert (PPO)	1515.36 ± 683.59	1407.36 ± 176.91	2637.27 ± 1757.72	122.09 ± 2.60	6129.10 ± 3491.47

6.2 Mujoco Tasks

We further test our method on five continuous control benchmarking Mujoco environments: Humanoid, Hopper, Walker2d and Swimmer and InvertedDoublePendulum. In this experiments, we still compare EBIL against GAIL, GMMIL and RED, where we employ Trust Region Policy Optimization (TRPO) [40] as the learning algorithm in the implementation for all evaluated methods. Expert agents are trained with OpenAI baselines version [7] of Proximal Policy Optimization (PPO) [41]. Furthermore, we consider to sample 4 trajectories by the trained expert policy, as [19, 46] do. The training curves are in Appendix C.4, showing the training stability of the algorithm.

As shown in Tab. 1, EBIL achieves the best or comparable performance among all environments, indicating that the energy is able to become an excellent fixed reward function and is efficient to guide the agent to do imitation learning. It is worth noting that we do not apply BC initialization for all tasks. And we are unsuccessful with GMMIL and RED on Swimmer even after extensive tuning.

7 Conclusion and Future Impacts

In this paper, we propose Energy-Based Imitation Learning (EBIL), which shows that it is feasible to compute a fixed reward function via estimating the expert energy to help agents learn from the expert demonstrations. We further theoretically discuss the connections of our method with Maximum Entropy Inverse Reinforcement Learning (MaxEnt IRL) and reveal that EBIL is a dual problem of MaxEnt IRL and provide a simplified and efficient solution. We empirically show the comparable or better performance of EBIL against state-of-the-art imitation learning algorithms in multiple tasks.

For potential impacts, EBIL simplifies the learning procedure and increase the efficiency of imitation learning, which can be applied into practical decision-making problems where agents are required to imitate demonstrated behaviors such as robotics and autonomous driving in the future work. However, advances in automation led by IL may bring about workers who are engaged in repetitive tasks being replaced by robots.

References

- [1] Pieter Abbeel and Andrew Y Ng. Apprenticeship learning via inverse reinforcement learning. In *Proceedings of the twenty-first international conference on Machine learning*, page 1, 2004.
- [2] Michael Bloem and Nicholas Bambos. Infinite time horizon maximum causal entropy inverse reinforcement learning. In *53rd IEEE Conference on Decision and Control*, pages 4911–4916. IEEE, 2014.
- [3] Rinu Boney, Juho Kannala, and Alexander Ilin. Regularizing model-based planning with energy-based models. *arXiv preprint arXiv:1910.05527*, 2019.
- [4] Kianté Brantley, Wen Sun, and Mikael Henaff. Disagreement-regularized imitation learning. In *International Conference on Learning Representations*, 2020.
- [5] Andrew Brock, Jeff Donahue, and Karen Simonyan. Large scale gan training for high fidelity natural image synthesis. *arXiv preprint arXiv:1809.11096*, 2018.
- [6] Yuri Burda, Harrison Edwards, Amos J. Storkey, and Oleg Klimov. Exploration by random network distillation. *CoRR*, abs/1810.12894, 2018.
- [7] Prafulla Dhariwal, Christopher Hesse, Oleg Klimov, Alex Nichol, Matthias Plappert, Alec Radford, John Schulman, Szymon Sidor, Yuhuai Wu, and Peter Zhokhov. Openai baselines (2017). URL <https://github.com/opffenai/baselines>, 2016.
- [8] Yilun Du and Igor Mordatch. Implicit generation and generalization in energy-based models. *CoRR*, abs/1903.08689, 2019.
- [9] Yilun Du and Igor Mordatch. Implicit generation and modeling with energy based models. In *Advances in Neural Information Processing Systems*, pages 3603–3613, 2019.
- [10] Chelsea Finn, Paul Christiano, Pieter Abbeel, and Sergey Levine. A connection between generative adversarial networks, inverse reinforcement learning, and energy-based models. *arXiv preprint arXiv:1611.03852*, 2016.
- [11] Chelsea Finn, Sergey Levine, and Pieter Abbeel. Guided cost learning: Deep inverse optimal control via policy optimization. In *International Conference on Machine Learning*, pages 49–58, 2016.
- [12] Seyed Kamyar Seyed Ghasemipour, Richard Zemel, and Shixiang Gu. A divergence minimization perspective on imitation learning methods. *arXiv preprint arXiv:1911.02256*, 2019.
- [13] Ian Goodfellow, Jean Pouget-Abadie, Mehdi Mirza, Bing Xu, David Warde-Farley, Sherjil Ozair, Aaron Courville, and Yoshua Bengio. Generative adversarial nets. In *Advances in neural information processing systems*, pages 2672–2680, 2014.
- [14] Michael Gutmann and Aapo Hyvärinen. Noise-contrastive estimation: A new estimation principle for unnormalized statistical models. In *Proceedings of the Thirteenth International Conference on Artificial Intelligence and Statistics*, pages 297–304, 2010.
- [15] Michael U Gutmann and Aapo Hyvärinen. Noise-contrastive estimation of unnormalized statistical models, with applications to natural image statistics. *Journal of Machine Learning Research*, 13(Feb):307–361, 2012.
- [16] Tuomas Haarnoja, Haoran Tang, Pieter Abbeel, and Sergey Levine. Reinforcement learning with deep energy-based policies. In *Proceedings of the 34th International Conference on Machine Learning-Volume 70*, pages 1352–1361. JMLR. org, 2017.
- [17] Tuomas Haarnoja, Aurick Zhou, Pieter Abbeel, and Sergey Levine. Soft actor-critic: Off-policy maximum entropy deep reinforcement learning with a stochastic actor. *arXiv preprint arXiv:1801.01290*, 2018.
- [18] Nicolas Heess, David Silver, and Yee Whye Teh. Actor-critic reinforcement learning with energy-based policies. In *EWRL*, pages 43–58, 2012.

[19] Jonathan Ho and Stefano Ermon. Generative adversarial imitation learning. In *Advances in neural information processing systems*, pages 4565–4573, 2016.

[20] Ahmed Hussein, Mohamed Medhat Gaber, Eyad Elyan, and Chrisina Jayne. Imitation learning: A survey of learning methods. *ACM Computing Surveys (CSUR)*, 50(2):21, 2017.

[21] Max Jaderberg, Wojciech M Czarnecki, Iain Dunning, Luke Marris, Guy Lever, Antonio Garcia Castaneda, Charles Beattie, Neil C Rabinowitz, Ari S Morcos, Avraham Ruderman, et al. Human-level performance in first-person multiplayer games with population-based deep reinforcement learning. *arXiv preprint arXiv:1807.01281*, 2018.

[22] Kee-Eung Kim and Hyun Soo Park. Imitation learning via kernel mean embedding. In *Thirty-Second AAAI Conference on Artificial Intelligence*, 2018.

[23] Ilya Kostrikov, Kumar Krishna Agrawal, Debidatta Dwibedi, Sergey Levine, and Jonathan Tompson. Discriminator-actor-critic: Addressing sample inefficiency and reward bias in adversarial imitation learning. *arXiv preprint arXiv:1809.02925*, 2018.

[24] Yann LeCun, Sumit Chopra, Raia Hadsell, M Ranzato, and F Huang. A tutorial on energy-based learning. *Predicting structured data*, 1(0), 2006.

[25] Yujia Li, Kevin Swersky, and Rich Zemel. Generative moment matching networks. In *International Conference on Machine Learning*, pages 1718–1727, 2015.

[26] KOICHI Miyasawa. An empirical bayes estimator of the mean of a normal population. *Bull. Inst. Internat. Statist.*, 38(181-188):1–2, 1961.

[27] Volodymyr Mnih, Koray Kavukcuoglu, David Silver, Andrei A Rusu, Joel Veness, Marc G Bellemare, Alex Graves, Martin Riedmiller, Andreas K Fidjeland, Georg Ostrovski, et al. Human-level control through deep reinforcement learning. *Nature*, 518(7540):529, 2015.

[28] Andrew Y Ng, Stuart J Russell, et al. Algorithms for inverse reinforcement learning. In *Icml*, volume 1, page 2, 2000.

[29] Erik Nijkamp, Mitch Hill, Song-Chun Zhu, and Ying Nian Wu. Learning non-convergent non-persistent short-run mcmc toward energy-based model, 2019.

[30] OpenAI. Openai five. <http://blog.openai.com/openai-five/>, 2018.

[31] Dean A Pomerleau. Efficient training of artificial neural networks for autonomous navigation. *Neural Computation*, 3(1):88–97, 1991.

[32] Martin Raphan and Eero P Simoncelli. Least squares estimation without priors or supervision. *Neural computation*, 23(2):374–420, 2011.

[33] Siddharth Reddy, Anca D. Dragan, and Sergey Levine. SQL: imitation learning via regularized behavioral cloning. *CoRR*, abs/1905.11108, 2019.

[34] Herbert Robbins. *An empirical Bayes approach to statistics*. Office of Scientific Research, US Air Force, 1955.

[35] Stéphane Ross and Drew Bagnell. Efficient reductions for imitation learning. In *Proceedings of the thirteenth international conference on artificial intelligence and statistics*, pages 661–668, 2010.

[36] Stéphane Ross, Geoffrey Gordon, and Drew Bagnell. A reduction of imitation learning and structured prediction to no-regret online learning. In *Proceedings of the fourteenth international conference on artificial intelligence and statistics*, pages 627–635, 2011.

[37] Brian Sallans and Geoffrey E Hinton. Reinforcement learning with factored states and actions. *Journal of Machine Learning Research*, 5(Aug):1063–1088, 2004.

[38] Saeed Saremi and Aapo Hyvarinen. Neural empirical bayes. *arXiv preprint arXiv:1903.02334*, 2019.

- [39] Saeed Saremi, Arash Mehrjou, Bernhard Schölkopf, and Aapo Hyvärinen. Deep energy estimator networks. *arXiv preprint arXiv:1805.08306*, 2018.
- [40] John Schulman, Sergey Levine, Pieter Abbeel, Michael Jordan, and Philipp Moritz. Trust region policy optimization. In *International conference on machine learning*, pages 1889–1897, 2015.
- [41] John Schulman, Filip Wolski, Prafulla Dhariwal, Alec Radford, and Oleg Klimov. Proximal policy optimization algorithms. *arXiv preprint arXiv:1707.06347*, 2017.
- [42] Yang Song, Sahaj Garg, Jiaxin Shi, and Stefano Ermon. Sliced score matching: A scalable approach to density and score estimation. *arXiv preprint arXiv:1905.07088*, 2019.
- [43] Umar Syed, Michael Bowling, and Robert E Schapire. Apprenticeship learning using linear programming. In *Proceedings of the 25th international conference on Machine learning*, pages 1032–1039. ACM, 2008.
- [44] Pascal Vincent. A connection between score matching and denoising autoencoders. *Neural computation*, 23(7):1661–1674, 2011.
- [45] Pascal Vincent, Hugo Larochelle, Yoshua Bengio, and Pierre-Antoine Manzagol. Extracting and composing robust features with denoising autoencoders. In *Proceedings of the 25th international conference on Machine learning*, pages 1096–1103. ACM, 2008.
- [46] Ruohan Wang, Carlo Ciliberto, Pierluigi Vito Amadori, and Yiannis Demiris. Random expert distillation: Imitation learning via expert policy support estimation. *CoRR*, abs/1905.06750, 2019.
- [47] Brian D Ziebart. *Modeling purposeful adaptive behavior with the principle of maximum causal entropy*. PhD thesis, figshare, 2010.
- [48] Brian D Ziebart, Andrew Maas, J Andrew Bagnell, and Anind K Dey. Maximum entropy inverse reinforcement learning. 2008.

A Algorithm

Algorithm 1 Energy-Based Imitation Learning

```

1: Input: Expert demonstration data  $\tau_E = \{(s_i, a_i)\}_{i=1}^N$ , parameterized energy-based model  $E_\phi$ , parameterized policy  $\pi_\theta$ ;
2: for  $k = 0, 1, 2, \dots$  do
3:   Optimize  $\phi$  with the objective in Eq. (12).
4: end for
   Compute the surrogate reward function  $\hat{r}$  via Eq. (13).
5: for  $k = 0, 1, 2, \dots$  do
6:   Update  $\theta$  with a normal RL procedure using the surrogate reward function  $\hat{r}$ .
7: end for
8: return  $\pi$ 

```

B Proofs

B.1 Proof of Proposition 2

Before showing the equivalence between the reverse KL divergence objective and the EBIL objective, we first present the following lemma.

Lemma 3 (Lemma 3 of [19]). *\overline{H} is strictly concave, and for all $\pi \in \Pi$ and $\rho \in \mathcal{D}$, we have $H(\pi) = \overline{H}(\rho_\pi)$ and $\overline{H}(\rho) = H(\pi_\rho)$, where $\overline{H}(\rho) = -\sum_{s,a} \rho_\pi \log \rho_\pi(s, a) / \sum_{a'} \rho(s, a')$ is the entropy of the occupancy measure.*

Proof of Proposition 2. Take Eq. (9) into Eq. (8) for both policy π and π_E , one can obtain that:

$$\begin{aligned}
D_{\text{KL}}(\rho_\pi \parallel \rho_{\pi_E}) &= \sum_{s,a} \rho_\pi(s, a) \log \frac{\rho_\pi(s, a)}{\rho_{\pi_E}(s, a)} \\
&= \sum_{s,a} \rho_\pi \left(\log \rho_\pi(s, a) - \log \frac{e^{-E_{\pi_E}(s, a)}}{Z'} \right) \\
&= \sum_{s,a} \rho_\pi (E_{\pi_E}(s, a) + \log \rho_\pi(s, a) + \log Z') \\
&= \mathbb{E}_\pi [E_{\pi_E}(s, a)] + \sum_{s,a} \rho_\pi \log \rho_\pi(s, a) + \text{const} \tag{19} \\
&= \mathbb{E}_\pi [E_{\pi_E}(s, a)] + \sum_{s,a} \rho_\pi \log \rho_\pi(s, a) - \log \sum_{s,a'} \rho(s, a') + \text{const} \\
&= \mathbb{E}_\pi [E_{\pi_E}(s, a)] + \sum_{s,a} \rho_\pi \log \left[\rho_\pi(s, a) / \sum_{a'} \rho(s, a') \right] + \text{const} \\
&= \mathbb{E}_\pi [E_{\pi_E}(s, a)] - \overline{H}(\rho_\pi) + \text{const} \\
&= \mathbb{E}_\pi [E_{\pi_E}(s, a)] - H(\pi) + \text{const} ,
\end{aligned}$$

where E_{π_E} is the EBM of policy π_E and Z' is its partition function. Thus, Eq. (8) in the end leads to the objective function of EBIL Eq. (10). \square

B.2 Proof of Proposition 3

Proof of Proposition 3. Similarly as in [19], we would like to relax Eq. (16) into the following form with the motivation from Eq. (6):

$$\min_{\pi} d_\psi(\rho_\pi, \rho_{\pi_E}) - H(\pi) , \tag{20}$$

where we modify the IRL regularizer ψ so that $d_\psi(\rho_\pi, \rho_{\pi_E}) \triangleq \psi^*(\rho_\pi - \rho_{\pi_E})$ is a smooth distance metric that penalizes violations in the difference between the occupancy measures. By choosing $\psi = \mathbb{E}_{\pi_E}[-1 - \log(r(s, a)) + r(s, a)]$, we obtain $d_\psi(\rho_\pi, \rho_{\pi_E}) = D_{\text{KL}}(\rho_\pi \| \rho_{\pi_E})$ ⁴. Thus we have:

$$\min_{\pi} D_{\text{KL}}(\rho_\pi \| \rho_{\pi_E}) - H(\pi). \quad (21)$$

Refer to Eq. (19), we have:

$$D_{\text{KL}}(\rho_\pi \| \rho_{\pi_E}) = \mathbb{E}_\pi [E_{\pi_E}(s, a)] - H(\pi) + \text{const}. \quad (22)$$

Thus, we can rewrite Eq. (21) as the following optimization problem:

$$\pi^* = \arg \max_{\pi} \mathbb{E}_\pi [-E_{\pi_E}(s, a)] + 2H(\pi), \quad (23)$$

which leads to the EBIL objective Eq. (10) with the temperature hyperparameter $\alpha = 2$. This indicates that EBIL is a dual problem of the MaxEnt IRL problem. \square

B.3 Proof of Proposition 4

Proof of Proposition 4. Suppose we have recovered the optimal reward function \hat{r} , then we can derive the objective of the KL divergence between the two trajectories into the forward MaxEnt RL procedure.

With chain rule, the induced trajectory distribution $p(\tau)$ is given by

$$p(\tau) = p(s_0) \prod_{t=0}^T P(s_{t+1}|s_t, a_t) \pi(a_t|s_t). \quad (24)$$

Suppose the desired expert trajectory distribution $p(\tau_E)$ is given by

$$\begin{aligned} p(\tau) &\propto p(s_0) \prod_{t=0}^T P(s_{t+1}|s_t, a_t) \pi(a_t|s_t) \exp(\hat{r}^*(\tau)) \\ &= p(s_0) \prod_{t=0}^T P(s_{t+1}|s_t, a_t) \pi(a_t|s_t) \exp\left(\sum_{t=0}^T \hat{r}^*(s_t, a_t)\right), \end{aligned} \quad (25)$$

now we will show that the following optimization problem is equivalent to a forward MaxEnt RL procedure given the optimal reward \hat{r}^* :

$$\begin{aligned} D_{\text{KL}}(p(\tau) \| p(\tau_E)) &= \sum_{\tau \sim \pi} p(\tau) \log \frac{p(\tau)}{p(\tau_E)} \\ &= \sum_{\tau \sim \pi} p(\tau) (\log p(\tau) - \log p(\tau_E)) \\ &= \mathbb{E}_{\tau \sim \pi} \left[\log p(s_0) + \sum_{t=0}^T (\log P(s_{t+1}|s_t, a_t) + \hat{r}^*(s_t, a_t)) - \right. \\ &\quad \left. \log p(s_0) - \sum_{t=0}^T T (\log P(s_{t+1}|s_t, a_t) + \log \pi(a_t|s_t)) \right] + \text{const} \\ &= \mathbb{E}_{\tau \sim p(\tau)} \left[\sum_{t=0}^T \hat{r}^*(s_t, a_t) - \pi(a_t|s_t) \right] + \text{const} \\ &= \sum_{t=0}^T \mathbb{E}_{(s_t, a_t) \sim \rho(s_t, a_t)} [\hat{r}^*(s_t, a_t) - \log \pi(a_t|s_t)] + \text{const}. \end{aligned} \quad (26)$$

⁴Full derivations can be found in Appendix D of [12] and we replace $c(s, a)$ with $-r(s, a)$.

Without loss of generality, we approximate the finite term $\sum_{t=0}^T \mathbb{E}_{(s_t, a_t)}$ with an infinite term \mathbb{E}_π by the definition, and then we have

$$\begin{aligned}
D_{KL}(p(\tau) \| p(\tau_E)) &\approx \mathbb{E}_{(s, a) \sim \rho(s, a)} [\hat{r}^*(s, a) - \log \pi(a|s_t)] + \text{const} \\
&= \mathbb{E}_\pi [\hat{r}^*(s, a) - \log \pi(a|s)] + \text{const} \\
&= \mathbb{E}_\pi [\hat{r}^*(s, a)] - \mathbb{E}_\pi [\log \pi(a|s)] + \text{const} \\
&= \mathbb{E}_\pi [\hat{r}^*(s, a)] - H(\pi) + \text{const} .
\end{aligned} \tag{27}$$

Thus the objective Eq. (18) is equivalent to the following optimization problem:

$$\max_{\pi} \mathbb{E}_\pi [\hat{r}^*(s, a)] + H(\pi), \tag{28}$$

which is exactly the objective of a forward MaxEnt RL procedure (Eq. (17)). This indicates that when MaxEnt IRL recovers the optimal reward function, a forward RL learning which leads to the optimal (expert) policy is equivalent to minimize the reverse KL divergence between the trajectories sampled by the agent and by the expert. \square

B.4 Proof of Proposition 5

Proof of Proposition 5. From the deviation Eq. (27), we know that the optimization problem Eq. (18) is equivalent to a forward MaxEnt RL problem Eq. (17). Let $r^*(s, a) = -E(s, a)$, and we will exactly get the EBIL objective Eq. (10). Note that the reverse KL divergence IL objective Eq. (8) can also be derived into the EBIL objective Eq. (10) followed Eq. (19). Thus Eq. (18) is equivalent to both the reverse KL divergence IL objective Eq. (8) and the EBIL objective Eq. (10). \square

C Experiments

C.1 Hyperparameters

We show the hyperparameters for both DEEN training and policy training on different tasks in Tab. 2. Specifically, we use MLPs as the network for training DEEN and the policy network.

Table 2: Important hyperparameters used in our experiments

	Hyperparameter	One-D.	Human.	Hop.	Walk.	Swim.	Invert.
Policy	Hidden layers	3	3	3	3	3	3
	Hidden Size	200	200	200	200	200	200
	Iterations	6000	6000	6000	6000	6000	6000
	Batch Size	32	32	32	32	32	32
DEEN	Hidden layers	3	3	3	4	3	3
	Hidden size	200	200	200	200	200	200
	Epochs	3000	3000	6000	500	1900	500
	Batch Size	32	32	32	32	32	32
	Noise Scale σ	0.1	0.1	0.1	0.1	0.1	0.1
	Reward Scale α	1	1	5	1	1	1000

C.2 Synthetic Task Training Procedure

We demonstrate more training slices of the synthetic task in this section.

We analyze the learned behaviors during the training procedure of the synthetic task, as illustrated by visitation heatmaps in Fig. 3. For each method, we choose to show four training stages from different training iterations. These figures provide more evidence that although GAIL can finally achieve good results, EBIL provides fast and stable training. By contrast, GMMIL and RED fail to achieve effective results during the whole training time.

C.3 Energy Evaluation

Since the loss function of DEEN cannot be directly used as an indicator to evaluate the quality of the learned energy network, we propose to evaluate the averaged energy value for expert trajectories

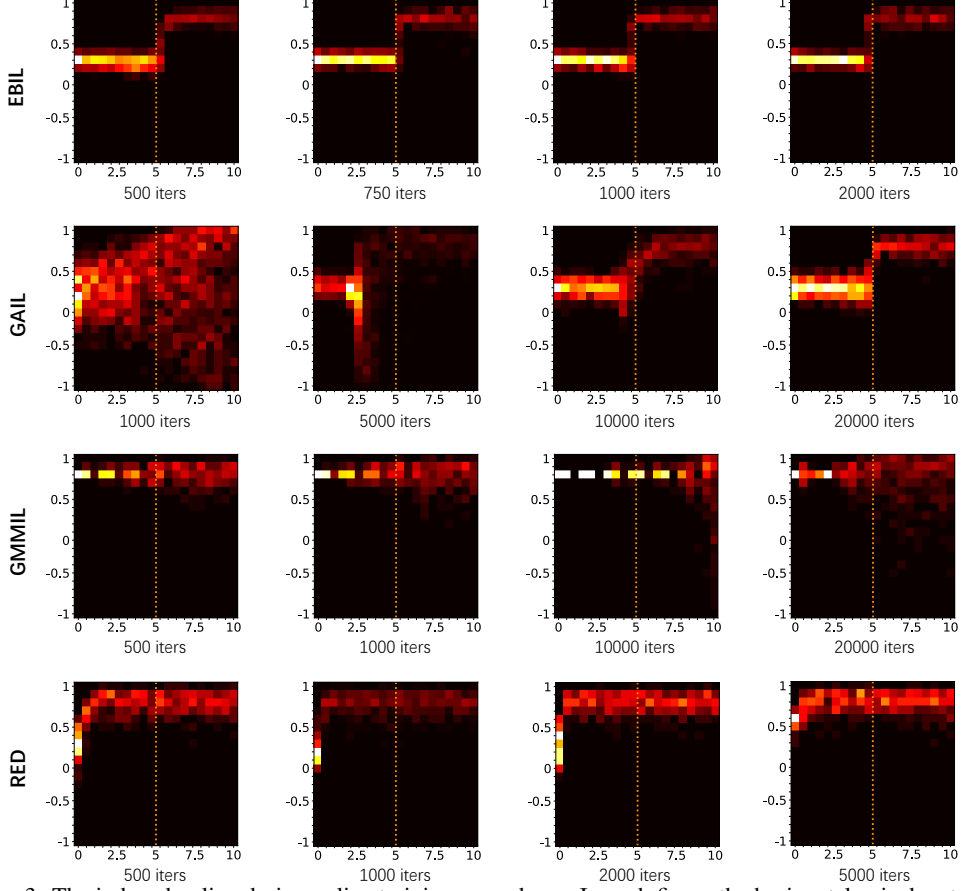


Figure 3: The induced policy during policy training procedures. In each figure the horizontal axis denotes the *state space*, and the vertical axis represents the *action space*. The brighter the yellow color, the higher the visitation frequency. Methods from top to bottom are separately EBIL, GAIL, GMMIL and RED and each one contains four training stages shown in one line.

and the random trajectories on different tasks. As shown in Fig. 4, DEEN finally converges in all experiments by differentiating the expert data. It is worth noting that in our experiments, we find that a well-trained energy network may be hard for agents to learn the expert policies on some environments. We regard it as the “sparse reward signals” problem, as discussed in Section 6.1. By contrast, sometimes a “half-trained” model may provide more smoother rewards, and can help the agent to learn more efficiently. Similar phenomenon also occurs when training the discriminator in GAN.

We will further analyze the training performance with energy models of different epochs in ablation study Section C.5.

C.4 Training Curves

We plot the episodes averaged return during the training procedure in Fig. 5, where EBIL shows effective guidance to help agent learn good policies while owns stability on all environments in comparison to the other methods. In our experiments, we find that the training procedure of GAIL suffers from instability.

C.5 Ablation Study

To further understand what the better energy model for learning a good policy is, we conduct ablation study on energy models trained from different epochs. The results are illustrated in Fig. 6, which verify our intuition that a “half-trained” model can provide smoother rewards that solve the “sparse reward” problem, which is better for imitating the expert policy.

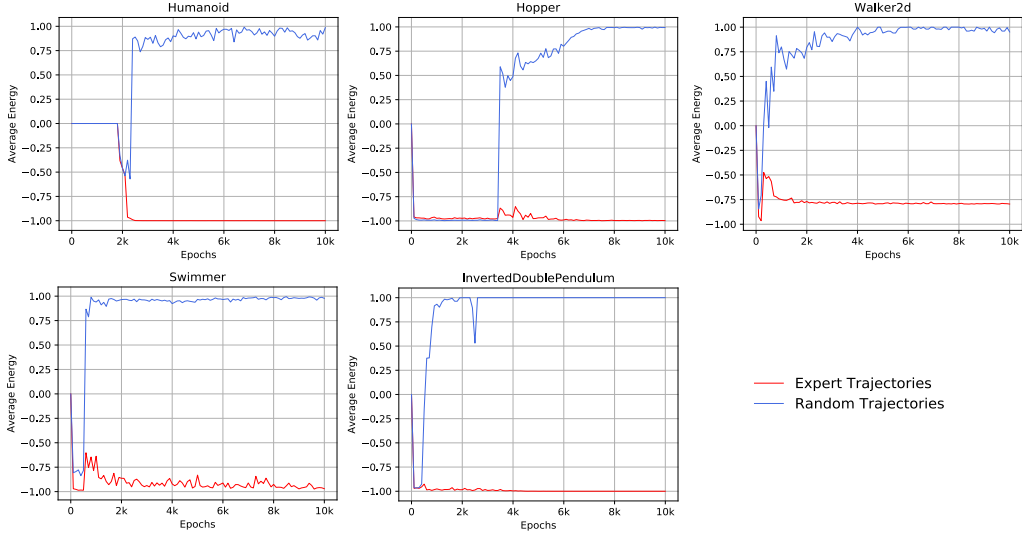


Figure 4: Energy evaluation curves on different mujoco tasks, where the red line represents for the average energy estimation on expert data and the blue is for random trajectories, which contain 100 trajectories separately. Note that lower energy values correspond to higher rewards. The min value is -1, and the max is 1 since we use \tanh for the last layer of the DEEN network.

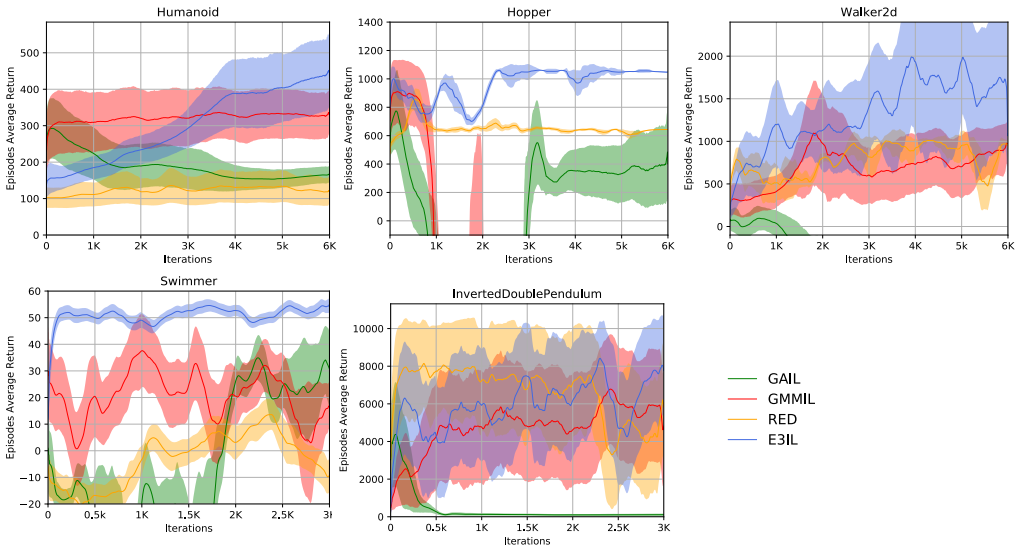


Figure 5: Training curves of GAIL, GMMIL, RED and EBIL on different continuous control benchmarking tasks, where the solid curves depict the mean and the shaded areas indicate the standard deviation. Each iterations contains 1024 timesteps.

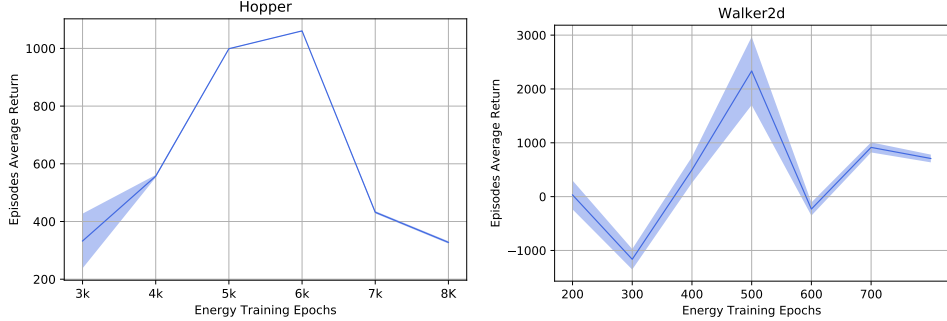


Figure 6: The average episode rewards evaluated on Hopper-v2 and Walker2d-v2 by agents that are learned with energy models from different training epochs.

D Further Discussions

D.1 Surrogate Reward Functions

As discussed in [23], the reward function is highly related to the property of the task. Positive rewards may achieve better performance in the “surviving” style environment, and negative ones may take advantage in the “per-step-penalty” style environment. The different choices are common in those imitation learning works based on GAIL, which can use either $\log(D)$ or $-\log(1 - D)$, where $D \in [0, 1]$ is the output of the discriminator, determined by the final “sigmoid” layer. In our work, we choose “*tanh*” as the final layer of the energy network, which in result leads the energy into a range of $[-1, 1]$. In order to adapt to different environments while holding the good property of the energy, we can apply a monotonically increasing linear function h as the surrogate reward function, which makes translation or scaling transformation on the energy outputs. It appears that in both of our environmental tasks, the original energy signal does not show much ascendancy, and thus we choose different h for these tasks.

In the one-dimension domain experiment, we choose to use the following surrogate reward function:

$$\hat{r}(s, a) = h(x) = x + 1, \quad (29)$$

where $\hat{r} \in [0, 2]$ and $x = -E(s, a)$ is the energy function. Thus, the experts’ state-action pair will get close-to-zero rewards at each step.

In mujoco tasks, we choose the surrogate reward function as:

$$\hat{r}(s, a) = h(x) = (x + 1)/2, \quad (30)$$

where $x = -E(s, a)$ is the energy function. Note that we construct this reward function to make a normalized reward $\hat{r} \in [0, 1]$ so that the non-expert’s state-action pair will gain near-zero rewards while the experts’ get close-to-one rewards at each step regarding the output range of the energy is $[-1, 1]$. In our experiments, similar rewards as the one-dimensional synthetic environment can also work well.

D.2 Discussions with MaxEnt RL Methods

Soft-Q Learning (SQL) [16] and Soft Actor-Critic (SAC) [17] are two main approaches of MaxEnt RL, particularly, they propose to use a general energy-based form policy as:

$$\pi(a_t | s_t) \propto \exp(-E(s_t, a_t)). \quad (31)$$

To connect the policy with soft versions of value functions and Q functions, they set the energy model $E(s_t, a_t) = -\frac{1}{\alpha} Q_{\text{soft}}(s_t, a_t)$ where α is the temperature parameter, such that the policy can be represented with the Q function which holds the highest probability at the action with the highest Q value, which essentially provides a soft version of the greedy policy. Thus, one can choose to optimize the soft Q function to obtain the optimal policy by minimizing the expected KL-divergence:

$$J(\pi) = \mathbb{E}_{s \sim \rho_{\mathcal{D}}^s} \left[D_{\text{KL}} \left(\pi(\cdot | s) \parallel \frac{\exp(Q(s, \cdot))}{Z(s)} \right) \right], \quad (32)$$

where $\rho_{\mathcal{D}}^s$ is the distribution of previously sampled states and actions, or a replay buffer. Therefore, the second term in the KL-divergence in fact can be regarded as the target or the reference for the policy.

Consider to use the KL-divergence as the distance metric in the general objective of IL shown in Eq. (3), then we get:

$$\pi^* = \arg \min_{\pi} \mathbb{E}_{\pi} [\text{D}_{\text{KL}} (\pi(\cdot|s) \| \pi_E(\cdot|s))] . \quad (33)$$

If we choose to model the expert policy using the energy form of Eq. (31) then we get:

$$\pi^* = \arg \min_{\pi} \mathbb{E}_{\pi} \left[\text{D}_{\text{KL}} \left(\pi(\cdot|s) \| \frac{\exp(-E_{\pi_E}(s, a))}{Z} \right) \right] . \quad (34)$$

Proposition 6. *The IL objective shown in Eq. (34) is equivalent to the EBIL objective shown in Eq. (10).*

Proof. Since Eq. (10) is equivalent to Eq. (8), it holds the optimal solution such that $\pi^* = \pi_E$ according to Proposition 1. Also, it is easy to see that Eq. (34) has the same optimal solution such that $\pi^* = \pi_E$. \square

Thus, Proposition 6 reveals the relation between MaxEnt RL and EBIL. Specifically, EBIL employs the energy model learned from expert demonstrations as the target policy. The difference is that MaxEnt RL methods use the Q function to play the role of the energy function, construct it as the target policy, and iteratively update the Q function and the policy, while EBIL directly utilizes the energy function to model the expert occupancy measure and constructs the target policy.

As a result, it makes sense to directly optimize the policy by taking the energy model as the target policy instead of the reward function, which leads to the optimal solution as:

$$\begin{aligned} \pi^*(a|s) &= \frac{\rho(s, a)}{\sum_{a'} \rho(s, a')} \\ &= \frac{\frac{1}{Z} \exp(-E(s, a))}{\frac{1}{Z} \sum_{a'} \exp(-E(s, a'))} \\ &= \frac{\exp(-E(s, a))}{\sum_{a'} \exp(-E(s, a'))} . \end{aligned} \quad (35)$$

Therefore, the optimal solution can also be obtained through estimating the energy function and summing it over the action space, which may be intractable for high-dimensional or continuous action space. Nevertheless, this can be solved in simple scenarios.